

Improving the Accuracy of the Calibration Method for Structured Light System

Nguyen Thi Kim Cuc*, Nguyen Van Vinh, Nguyen Thanh Hung, Nguyen Viet Kien

Hanoi University of Science and Technology, No. 1, Dai Co Viet, Hai Ba Trung, Hanoi, Viet Nam

Received: August 10, 2017; Accepted: May 25, 2018

Abstract

In a structured light system, calibration is an important step for estimating the intrinsic and extrinsic parameters of the camera and projector. System calibration errors directly affect the measurement errors. Therefore, the accurate calibration is the main prerequisite for a successful and accurate surface reconstruction. In this paper, the effect of checker size and checkerboard angle on the accurate calibration for a structured light system is presented. Relations between calibration error and checker size, fitting plane error and checkerboard angle are also studied. The purpose of the research is to achieve high accuracy when calibrating the system, by selecting the optimum checker size and determining the limited checkerboard angle $\Delta\beta$ in the whole volume of measurement $200(H)\times 250(W)\times 100(D)\text{mm}^3$

Keywords: Structured light system, 3D Surface Measurement, Calibration.

1. Introduction

Structured light measurement system (SLMS), has been widely used in the fields of artworks preservation, entertainment, security and medicine. Featuring high speed, ease of use, accuracy and flexibility than most of its competitors at a lower cost, this technique is only impeded by its cumbersome calibration process. [1]

For any SLMS, its accurate calibration is one of the key determinant factors for final accurate 3D measurement. Over the years, researchers have developed numerous approaches to calibrate these systems. The difference among those methods is usually between achievable accuracy and calibration complexity. There are attempts to calibrate exact system parameters (i.e., position and orientation) for both camera and projector [2]. Although these methods might be accurate, complicated and time-consuming calibration process is required.

For the SLMS, both reference-plane-based method [3], [4] and geometric calibration method [5], [6], [7] are extensively applied. The former can achieve good accurate calibration in a small scale if the system is properly configured. The latter tends to be more popular recently because open-source calibration software packages can be directly implemented to achieve great accuracy.

A flexible technique is proposed [8] that utilizes a planar checkerboard as calibration artifact. The camera calibration parameters are calculated using the

relation between the checker corners found on a camera coordinate system and a world coordinate system attached to the checkerboard plane. In [9], the optimal checker size for accurate calibration system, however, it lacks of accuracy in checkerboard position and orientation checkerboard, and the correlation between calibration error and checker size have not been studied.

In our research, the calibration procedures follow D. Moreno and G. Taubin method [10]. Where the camera, the projector and the geometric relationship between them are calibrated. The corner detection accuracy relies on the size of the checkerboard and the angle between checkerboard plane and the plane passes through the camera optical axis (checkerboard angle). Therefore, the checkerboard selection and allowable limit checkerboard angle are essential to calibrating the structured light system accurately.

2. Calibration principle

2.1. The system principle.

The simplest structured light system consists of a camera and a projector in Fig.1. $(o^w; x^w, y^w, z^w)$ denotes world coordinate system is attached to the checkerboard plane; $(o^c; x^c, y^c, z^c)$ and $(o^p; x^p, y^p, z^p)$ represent the camera and the projector coordinate systems respectively. The 2D target is the standard black and white checkerboard. In this research, the projector can be captured images like a camera, therefore calibrating the projector is in a similar manner as calibrating a camera.

* Corresponding author: Tel.: (+84) 966.078.567
Email: cuc.nguyenthikim@hust.edu.vn

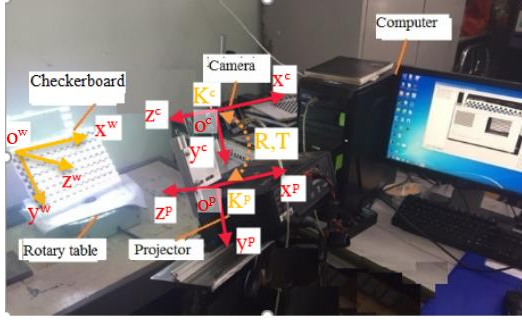


Fig. 1 Setup calibration structured light system and schematic diagram of world coordinate system ($O^w; x^w, y^w, z^w$), camera coordinate system ($O^c; x^c, y^c, z^c$), projector coordinate system ($O^p; x^p, y^p, z^p$).

Camera and projector both are used the pinhole model extended with radial and tangential distortion, with intrinsic parameters including focal length, principal point, pixel skew factor, and pixel size; A 3D point (x, y, z) expressed in the world coordinate system is first projected on to a point (u, v) in the image plane can be described using the following equation [8]:

$$s[u, v, 1] = A[R, t][x, y, z, 1], \quad (1)$$

where s is a scale factor. R is a 3×3 rotation matrix, and t is a 3×1 translation vector. $[R, t]$ represents extrinsic parameter of the system. A is camera and projector intrinsic matrices and can be expressed as:

$$A = \begin{bmatrix} f_u & \gamma & u_0 \\ 0 & f_v & v_0 \\ 0 & 0 & 1 \end{bmatrix}, \quad (2)$$

where (u_0, v_0) is the coordinate of principle point in the imaging sensor plane, the intersection between the optical axis and the imaging sensor plane, f_u and f_v are focal lengths along u and v axes of the image plane, and γ is the the skewness of two image axes.

The camera (or projector) lens can have nonlinear lens distortion K^c (or K^p), which can be described as a vector of five elements [8]:

$$K = [k_1 \quad k_2 \quad p_1 \quad p_2 \quad k_3]^T, \quad (3)$$

which is mainly composed of radial distortion coefficients $k_1, k_2,$ and k_3 , and tangential distortion coefficients $p_1,$ and p_2 , they can be corrected using the following formula:

$$\begin{cases} u' = u + (u - u_0) \left(\begin{array}{l} k_1 r^2 + k_2 r^4 + k_3 r^6 \\ + [2p_1 uv + p_2 (r^2 + 2u^2)] \end{array} \right) \\ v' = v + (v - v_0) \left(\begin{array}{l} k_1 r^2 + k_2 r^4 + k_3 r^6 \\ + [2p_1 uv + p_2 (r^2 + 2v^2)] \end{array} \right) \end{cases}, \quad (4)$$

Here, (u, v) and (u', v') are the camerar (or projector) point coodinate before and after correction, and $r = \sqrt{u^2 + v^2}$ denotes the Euclidean distance between the camera (or projector) point and the origin.

The projection describes a nonlinear 2 vector fuction $\Phi(x, y, z) = (\phi_u, \phi_v)$ [12] calculated over the intrinsic and extrinsic parameters. The parameters of Φ can be recovered from a set of correspondence points (from world points (x, y, z) to image points (u, v) captured from multiple views). The calibration error E of each model: camera calibration error E^c , projector calibration error E^p and stereo calibration error E^s is a combination of two factors in horizontal E_u and vertical E_v directions using:

$$\begin{cases} E = \sqrt{E_u^2 + E_v^2} \\ E_u = \Phi_u - u, E_v = \Phi_v - v \end{cases} \quad (5)$$

2. 2. Calibration processing

Selecting checkerboard size, the corner detection accuracy depends on the checker size of the checkerboard, thereby the size of checker squares significantly affects the accuracy of the estimated parameters. As a result, the calibration accuracy is influenced by the selection of the checkerboard size. The 15 different checker sizes are used. The range of checker plane is 180×180 mm. Checkerboard is generated with N rows and columns arranged in two alternating white and black squares, and the square size is S . Calculation each size checkerboard is $N \times S = 35 \times 5, 24 \times 7.5, 22 \times 8.2, 20 \times 9, 18 \times 10, 16 \times 11.25, 15 \times 12, 14 \times 12.8, 13 \times 13.8, 12 \times 15, 11 \times 16.4, 10 \times 18, 9 \times 20, 7 \times 26, 6 \times 30$.

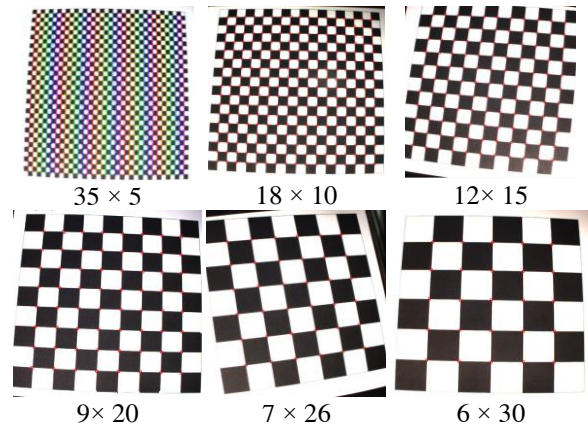


Fig. 2 Extract corner procedures of some checkerboard sizes.

The key to accurate reconstruction of the 3D shape is the proper calibration of each element used in the structured light system. For the camera distortion measurement, project a sequence of gray code combining phase shift pattern onto a static planar checkerboard place within the working volume ($H \times W \times D$). Capture one image for each pattern. Repeat this step for 10 checkerboard poses until properly cover all the working volume. With all these calibration parameters estimated from different checker size. In the reseach, the 3D scanning software

is written in C++ by visual studio 2015 using OpenCV 3.2 library [13]. The intrinsic parameters of the camera and the projectors are estimated using OpenCV's findChessboardCorners function and calling the function cornerSubPix() to automatically find sub-pixel checker corners locations.

Checkerboard angle estimation, as shown in Fig. 3, a stable to change checkerboard angles are used, the checkerboard size 12x12x15 to value these angles are used. The β is checkerboard angle. The allowable limited angle is $\Delta\beta$.

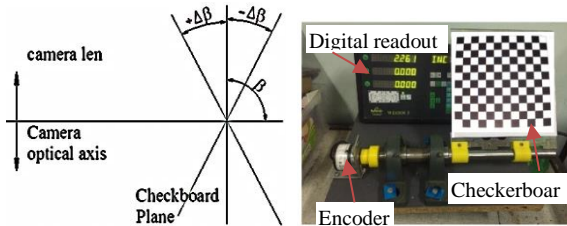


Fig. 3 Diagram and model of the checkerboard angle estimation.

All these calibration parameters from different checkerboard angles are estimated, a flat surface is then measured to compare the measure data. The measured surface is fitted to an ideal flat plane function. The fitting software is written by Matlab software R2015a×64. Once the plane is fitted, the measurement error can be estimated as follows:

$$z = Ax + By + C, \quad (6)$$

After obtaining the fitting plane, the error map can be gotten, which is orthogonal distance from any measurement points of reconstruction plane $p(x_i, y_i, z_i)$ to fitting plane, which is:

$$d = \frac{|Ax+By+C-z|}{\sqrt{A^2+B^2+1}}, \quad (7)$$

Assume there are n number of measurement points then fitting error F can calculate:

$$F = \sqrt{\frac{\sum_1^n d_i^2}{n}}, \quad (8)$$

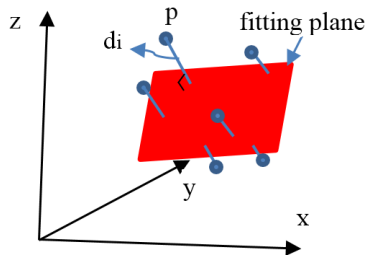


Fig. 4 Distance from 3D measurement points to the fitting plane.

Fig. 4 shows the collected 3D data fitted into an idea plane in the least squares algorithm [14]. The

fitting error result is analyzed as follow the second experiment.

3. Experiment result and discussion

Fig. 1 shows a picture of the system setup. This measure system contains a projector (InForcus N104) with a resolution 1280 × 960 pixels. It has a micromirror pitch of 7,6 μm. The camera used in this system is (DFK 41BU02) with an image resolution 1280 × 960 and a sensor size of 4.65 μm×4.65 μm. The lens used for the camera with a focal length of 12 mm and a high-speed computer.

A high-quality calibration is dependent on the accuracy of the dimensions of the calibration panel and the mark on it. To evaluate the calibrate accuracy in this research, two experiments were done with the structured light system.

The calibration method base on the printed pattern affixed to a flat surface is used in this experiment. The world coordinate system can establish based on one checkerboard set with its x, y axes on the plane and z axis perpendicular to the plane and pointing toward the system. The whole volume of the calibration board poses was around 200(H)×250(W)×100(D) mm³.

The first experiment, After a successful calibration, the output will show calibration error E using Equation (4) consist: the camera calibration error E^c , projector calibration error E^p and stereo calibration error E^s . One of the calibration result is presented in Fig. 5 using 3D scanning software.

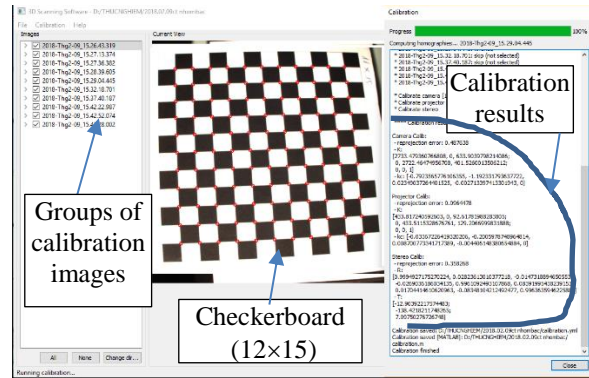


Fig. 5 Calibration result of checkerboard (12×15).

After capturing 10 groups of calibration images, the intrinsic and extrinsic parameters are estimated based on the same pose image for different checkerboards. Table 2 show a typical calibration results of the system. Calibration intrinsic results of camera A^c (pixels) are obtained as:

$$A^c = \begin{bmatrix} 2642.3173 & 0 & 668.2549 \\ 0 & 2641.8208 & 403.1572 \\ 0, & 0 & 1 \end{bmatrix}$$

Camera len distortion

$$K^c = [-0.7458 \quad 0.4419 \quad 0.0088 \quad -0.0058 \quad 0]$$

The projector calibration parameters $A^p(\text{pixels})$ are also obtained:

$$A^p = \begin{bmatrix} 337.0336 & 0 & 74.7179 \\ 0 & 667.598 & 232.3109 \\ 0, & 0 & 1 \end{bmatrix}$$

Projector len distortion

$$K^p = [-0.3360 \quad 1.5413 \quad -0.0288 \quad -0.0007 \quad 0]$$

Extrinsic parameters matrix

$$R = \begin{bmatrix} 0.9988 & 00.0121 & 0.0469 \\ -0.0151 & 0.9977 & 0.0648 \\ -0.0460 & -0.0655 & 0.9967 \end{bmatrix}$$

$$T = [-3.5367 \quad -133.0754 \quad 14.9471]$$

The relation between checker size is established and calibration errors (E^c , E^p , E^s) are shown in Fig. 6.

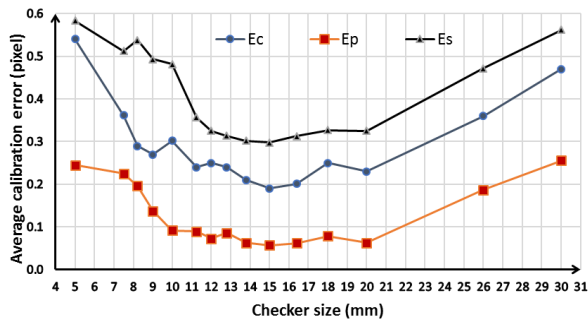


Fig. 6 Graph of the relation between checker size and calibration errors.

Because the size of the checkerboard table is fixed: When the checker size S is increased from 16 to 30 mm, the number of corners will be decreased from 100 to 36. However, when the checker size S is decreased from 15 to 5 mm, the number of corners will be increased from 144 to 1225. As shown in the Fig.6, the checker size is too large or too small leads to less accuracy calibration, which were caused by the checker point finding uncertainty because of the lack of feature point used and the lens distortion. Thus, there exists an optimal point where the two elements E_u and E_v are balanced, so that the calibration error is minimal. When the checkerboard size 15 mm and 121 corners, from Fig.6 can be seen the desire calibration errors are achieved: $E^c = 0.190$ (pixels), $E^p = 0.057$ (pixels), and $E^s = 0.298$ (pixels). This experiment demonstrated that indeed there is an optimal size of checkerboard in the established

working volume to the calibration of structured light system.

(F) Fitting plane (M) Measured point clouds

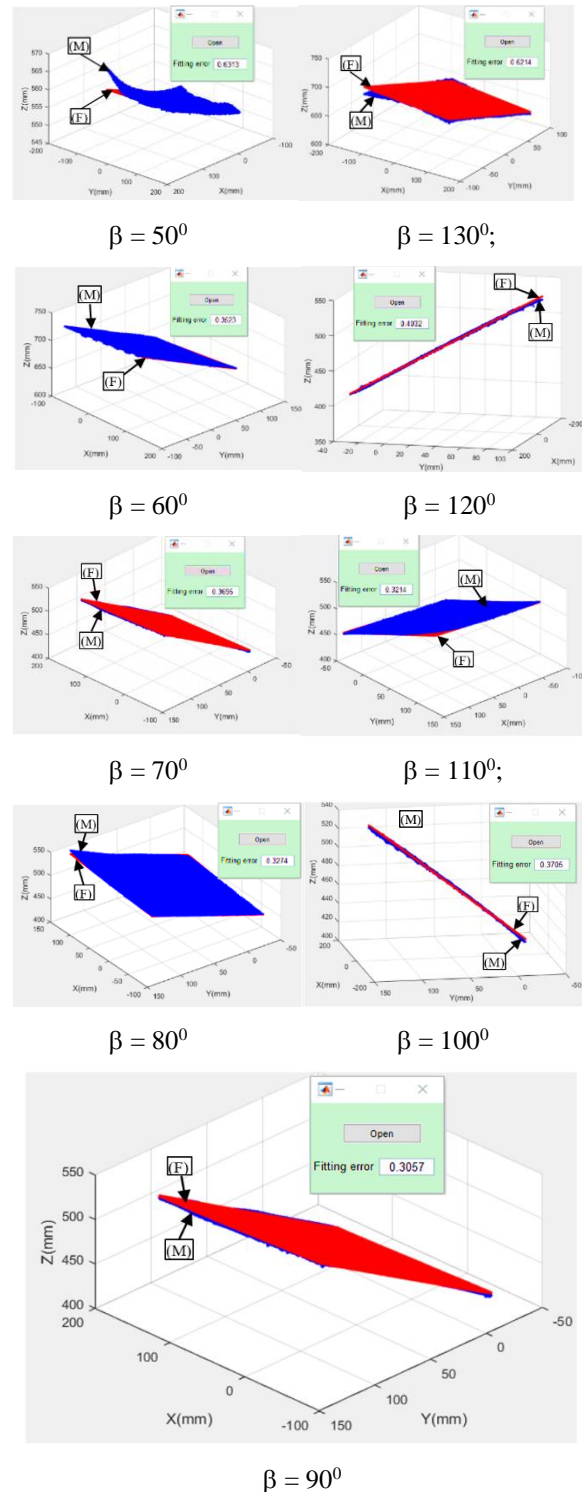


Fig. 7 The fitting plane results of 3D measured point clouds.

The second experiment, evaluate the checkerboard angle is as shown in Fig.7.

A plane checkerboard is using to evaluate the checkerboard angle. By fitting the measured coordinates to a fitting plane and calculating the distances between the measured points and the fitting plane, we found the measurement error of each point cloud after removing noise of measurement point clouds.

The Fig. 7 shows the effect of checkerboard angle to measured point clouds, the fitting results change when the checkerboard angles change. At angles of $\beta = 50^\circ$ and $\beta = 130^\circ$, the deviation between the measuring plane and the fitting plane are large and the fitting error decreases as the angle of deviation decreases and the smallest is at 90° . In the each case, the fitting error occur near the edges.

The relationship between the checkerboard angle and the fitting error is shown and evaluated in the Fig. 8.

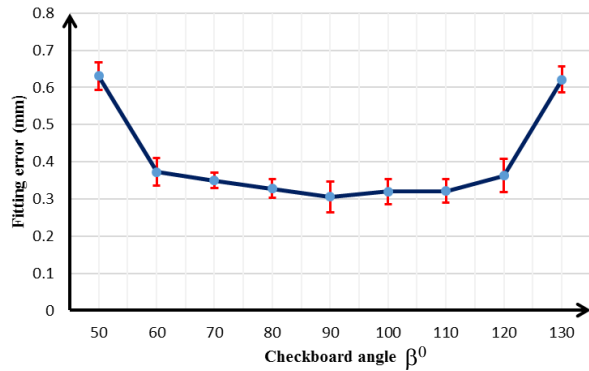


Fig. 8 Graph of the relation between checkerboard angle and fitting error.

The allowable limited angle $\Delta\beta$ is in the range of $\Delta\beta = \pm 30^\circ$, the measurement plane is quite flat and the fitting error is smaller than 0.4 mm. In a typical case, fitting errors are between 0.1 and 0.5 mm.

If the result displays a large fitting error consider readjusting the system, capturing additional checkerboard angle, or disabling some of the captured checkerboards which are out of the limited angle. That because, if the camera optical axis is perpendicular to the checkerboard plane (camera image plane is parallel to the checkerboard plane $\Delta\beta \sim 0$), the image pixels are square, and the checker points can be accurately determined. If the angle of the primary axis of the camera is not perpendicular to the plane of the checkerboard plane ($\Delta\beta$ is larger), the square will appear trapezoidal in the resulting image. It was caused by lens distortion.

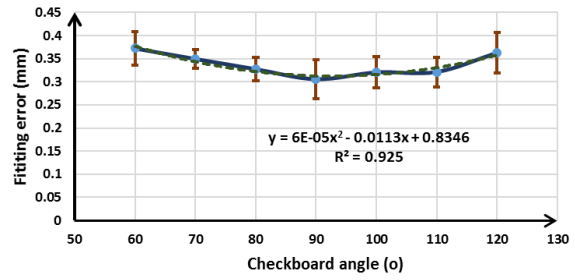


Fig. 9 The relation between β and F in $\Delta\beta$

The relation between checkerboard angle and fitting plane is present in Fig.9.

To demonstrate the effect of calibration accuracy on surface reconstruction accuracy, an object to verify the accuracy of the presented triangulation method was applied. The 3D object is reconstructed in two cases: case (a), calibration results with checkerboard angle inside $\Delta\beta$ and case (b), calibration results with checkerboard outside $\Delta\beta$. Calibration results are given in table 1:

Table. 1 Calibration result in two cases (a) and (b)

Calibration Results	(a)	(b)
Camera calibration error (pixels)	0.284	0.720
Projector calibration error (pixels)	0.324	0.415
Stereo calibration (pixels)	0.237	0.795

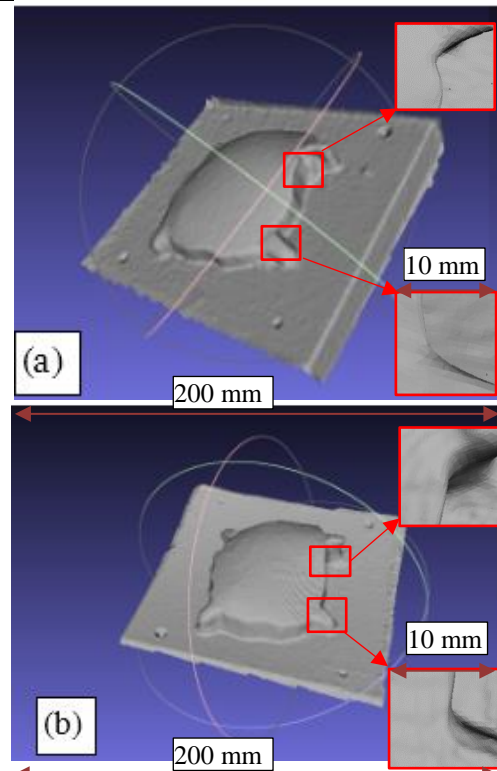


Fig. 9 Reconstruction of object and small details: (a) with angles in allowable limited angle (b) with some angles allowable limited angle

Calibration result in case (a) smaller than (b) so that the reconstruction result in case (b).

Finally, we scanned a mold from five different viewpoints and, after manual alignment and merging, we created a 3D model using MeshLab software. Fig. 10 shows the result of reconstruction 3D point cloud of the surface with the calibration in (a) and (b).

As shown in the Fig. 9, in the case (a) the plane of mould is flatter, and surface details are smoother than case (b). In the (b) the plane is bended down, the maximum relative error is 0,12% on the length 125 (mm). The result 3D reconstruction shows that the calibration accuracy affects the 3D reconstruction accuracy of the objects.

4. Conclusion

In this paper, the fitting software was built to value measurement error of reconstruction checkerboard plane. Two experiment was performed with our structured light system. The result showed that with the checker size in 15 mm and the checkerboard angle is in the allowable limit angle of $\Delta\beta = \pm 30^\circ$ in the working volume $200(H)\times 250(W)\times 100(D)$ mm³ our system achieved high calibration accuracy and measure accuracy. Experiment results show how the checker size and checkerboard angle affect the calibration accuracy, and estimated relation between them.

Acknowledgments

This work was supported by the 911 program of Ministry Education and Training.

References

- [1] J. Ma, X. Liu, X. Zhang, Z. Zhang, and Q. Zhao, 'High Accuracy and Low Cost 3D Surface Acquisition Using Structured Light', *Int. J. Adv. Comput. Technol.*, vol. 5, no. 9, pp. 1191–1201, 2013.
- [2] P. S. Huang, 'Calibration of a three-dimensional shape measurement system', *Opt. Eng.*, vol. 42, no. 2, p. 487, 2003.
- [3] J. Villa, M. Araiza, D. Alaniz, R. Ivanov, and M. Ortiz, 'Transformation of phase to (x,y,z)-coordinates for the calibration of a fringe projection profilometer', *Opt. Lasers Eng.*, vol. 50, no. 2, pp. 256–261, 2012.
- [4] Y. Xiao, Y. Cao, and Y. Wu, 'Improved algorithm for phase-to-height mapping in phase measuring profilometry.', *Appl. Opt.*, vol. 51, no. 8, pp. 1149–55, 2012.
- [5] H. Luo, B. Gao, J. Xu, and K. Chen, 'An approach for structured light system calibration', 2013 IEEE Int. Conf. Cyber Technol. Autom. Control Intell. Syst. IEEE-CYBER 2013, pp. 428–433, 2013.
- [6] Z. Li, Y. Shi, C. Wang, and Y. Wang, 'Accurate calibration method for a structured light system', *Opt. Eng.*, vol. 47, no. 5, p. 53604, 2008.
- [7] P. S. H. Song, Zhang, 'Novel method for structured light system calibration', *Opt. Eng.*, vol. 45, no. 8, p. 83601, 2006.
- [8] Z. Zhang, 'A Flexible New Technique for Camera Calibration (Technical Report)', *IEEE Trans. Pattern Anal. Mach. Intell.*, vol. 22, no. 11, pp. 1330–1334, 2002.
- [9] W. F. Lohry, 'Optimal checkerboard selection for structured light system calibration', *Mechanical Engineering Conf. Presentations, Papers, and Proceedings Mechanical*, 2009.
- [10] D. Moreno and G. Taubin, 'Simple , Accurate, and Robust Projector-Camera Calibration', *3D Imaging, Model. Process. Vis. Transm.*, vol. IEEE, no. 2012, pp. 464–471.
- [11] F. Ke, J. Xie, and Y. Chen, 'A flexible and high precision calibration method for the structured light vision system', *Optik (Stuttg.)*, vol. 127, no. 1, pp. 310–314, 2016.
- [12] C. Y. Chen and H. J. Chien, 'An incremental target-adapted strategy for active geometric calibration of projector-camera systems', *Sensors (Switzerland)*, vol. 13, no. 2, pp. 2664–2681, 2013.
- [13] G. Bradski, "The OpenCV Library," *Dr. Dobb's Journal of Software Tools*, 2000. [Online]. Available: <http://opencv.org/>
- [14] J. Allison, "Least Squares Data Fitting in MATLAB," 2010. [Online]. Available: <http://www.mathworks.com>